TRANSPLANT INTERNATIONAL

Transplant International ISSN 0934-0874

ORIGINAL ARTICLE

Invariant natural killer T cells infiltrate intestinal allografts undergoing acute cellular rejection

Tatsuaki Tsuruyama,[1,2] Yasuhiro Fujimoto,[3] Yukihide Yonekawa,[3] Masashi Miyao,[2] Hisashi Onodera,[4] Shinji Uemoto[3]* and Hironori Haga[1]*

1 Department of Diagnostic Pathology, Graduate School of Medicine, Kyoto University Hospital, Kyoto, Japan
2 Department of Forensic Medicine and Molecular Pathology, Graduate School of Medicine, Kyoto University Hospital, Kyoto, Japan
3 Department of Transplantation and Immunology, Kyoto University Hospital, Kyoto, Japan
4 Department of Surgery, St. Luke's International Hospital, Tokyo, Japan

Keywords
intestinal transplantation, acute cellular rejection, natural killer T cell.

Correspondence
Tatsuaki Tsuruyama, Kyoto University Hospital, 54, Shogoin-Kawahara-cho, Sakyo-ku, Kyoto 606-8397, Japan.
Tel.: 81-75-751-3488;
fax: 81-75-761-9591;
e-mail: tsuruyam@kuhp.kyoto-u.ac.jp

Conflicts of Interest
The authors have declared no conflicts of interest.

*These authors contributed equally to this research.

Received: 18 December 2011
Revision requested: 15 January 2012
Accepted: 27 January 2012
Published online: 1 March 2012

doi:10.1111/j.1432-2277.2012.01450.x

Summary

Immunological responses in human intestinal allografts are poorly understood and accurate diagnosis of acute cellular rejection remains difficult. Here, human intestinal allografts were analyzed by multi-color quantitative fluorescent immunohistochemical morphometry in order to monitor the clinical course of rejection. Morphometry gave two-dimensional plots based on size and circularity, and identified phenotypes of individual cells infiltrating the allograft by fluorescent staining. Using this method, invariant TCRVα24$^+$ NKT (iNKT) cells were observed in the intestinal allograft during rejection. Because these were not identified in the normal donor intestine before surgery, this finding was considered to be a signature of acute cellular rejection of the intestinal allograft. Infiltrating iNKT cells released IL-4 and IL-5, Th2-related cytokines that antagonize the Th1 responses that induce acute cellular rejection. Histological observation suggested eosinophilic enteritis in the mucosa with elevation of IL-4 and IL-5. In conclusion, iNKT cells were recruited to the intestine; however, because higher levels of IL-4 and IL-5 may contribute to eosinophilic enteritis, timely steroid administration is recommended for allograft injury due to enteritis, as well as acute cellular rejection.

Introduction

Intestinal transplantation is a commonly accepted standard therapy for patients with irreversible parenteral nutrition complications following intestinal failure or short-bowel syndrome [1–3]. In recent years, the 1-year patient survival has improved, and it is now possible for more than half of children who survive a transplant to be weaned off parenteral nutrition [4]. However, acute cellular rejection (ACR) remains the major cause of intestinal graft failure after transplantation, and for most patients with severe acute rejection, sufficient recovery of mucosal absorption function remains difficult [5].

Histological diagnosis is a reliable and sensitive method for detecting rejection. The major histological finding of acute rejection is mixed inflammatory cell infiltrate, including activated large lymphocytes and crypt apoptosis [6–8]. In the present study, we applied an established grading system developed by a Pittsburgh University Group [6], and we delineated immune responses in the allograft with reference to clinical and immunological data and inflammatory cytokine production. The objective of this study was to precisely evaluate specific immune responses.

We focused on the behavior of invariant TCRVα24$^+$ NKT (iNKT) cells in the intestinal allograft. iNKT cells share the characteristics of both T and natural killer cells, and constitute a unique class of the T lymphocyte lineage

[9]. They have a very restricted T cell receptor (TCR) repertoire consisting of an invariant Vα24-Ja18 chain (formerly Va24-JaQ) paired with a Vβ11 chain in human peripheral blood [10–12]. Human iNKT cells can be activated by glycolipid antigens, such as beta-galactosylceramide and iGb3, which are presented by CD1d expressed in dendritic cells [13]. When activated, iNKT cells immediately produce large amounts of pro-inflammatory T helper 1 cytokines [e.g., IFN-γ and tumor necrosis factor (TNF)-α] and anti-inflammatory T helper 2 cytokines (e.g., IL-4, IL-10, and IL-13). An experimental study demonstrated that NKT cells are required in the induction of allograft tolerance [14]. We previously reported human iNKT cells in the normal colon, and that iNKT cell infiltration is one of the prognostic factors of colorectal cancer [15]. On the other hand, intestinal NKT cells are diverse, while iNKT cells are rare [16]. However, we were able to identify iNKT cells in the intestinal allograft during acute cellular rejection.

Here, we aimed to identify and investigate the roles of iNKT cells in intestinal allograft rejection and to understand the immunological features of intestinal allografts. For quantitative morphometric analysis, we developed a multi-color system to measure the degree of circularity, which is able to evaluate the intensity of labeled stained antigens in individual objective cells. iNKT cells were identified and analyzed quantitatively using this system. The methodology used in this study is described in detail below.

Materials and methods

Case selection

From May 1996 to February 2010, eight children underwent orthotopic intestinal transplantation at Kyoto University Hospital [17]. These patients were assessed by routine endoscopic biopsy for 2 months after transplantation in order to monitor for ACR (Table 1). The remaining patient did not undergo routine biopsy because the methodology of morphometric analysis was not established or because the patient's condition was not stable. The study was performed with the comprehensive written informed consent of the patients' parents for a clinical study that was approved by the Committee of Medical Ethics of the Graduate School of Medicine, Kyoto University. The analyzed histologic specimens were biopsied only for pathological diagnosis by immunohistochemistry and routine staining. We obtained written informed consent from all participants (or the patients' mothers) involved in our study, including the five donors.

Patients had segments of small intestine engrafted from living donors due to the presence of short-gut syndrome secondary to surgical removal of a large portion of the ileum. When patients complained of fever (>37 °C) and

Table 1. Profiles of patients and donors.

Patient (ID)	Patient age (y)/gender	Donor age (y)/gender	Relation of donor to the patient	Histology of ACR					Reolved status (post-operative date)	Etiology of transplantation	Transplant	Steroid pulse at ACR (mg/kg/day)
				Post-operative date of ACR	Apoptotic crypt count	Epithelial injury	Inflammation	Histological grade of ACR				
1	2/M	20–30/F (mother)	Mother	12	8.5	Ulceration	sev	sev	23	RA+SB	Ileum	30
2	0(8 weeks)/F	20–30/F (mother)	Mother	12	6.1	absent	mod	mild	15	RA+SB	Ileum	30
				18	6.3	absent	mild	mild	19			
				20, 22, 23	6.2	absent	mild	mild	23			
				25, 27, 28	6.3	absent	mild	mild	28			
3	4/M	20–30/F	Mother	66	6.1	mild/ scant	absent	mild	66	Hir	Ileum	30
4	4/F	20–30/F	Brain-death donor	22	7.5	cryptitis	sloughing	mild	23	RA+SB	Ileum	30
				95	7.2	sloughing	mod	mild	100			
5	1/F	20–30/F	Mother	11	8.5	sloughing	sev	sev	23	RA+SB	Ileum	30
6	12/F	20–30/F	Mother	27	6.2	absent	absent	mild	32	RA+SB	Ileum	30
7	19/M	40–50/M	Brain-death donor	12	6.4	absent	mild	mild	12	Hir	Ileum	15
8	7/F	30–40/M	Father	11	6.5	absent	absent	mild	12	RA+SB	Ileum	30

M, male; F, female; Apoptotic crypt count (per 10 crypts); ACR, acute rejection. Inflammation and ACR grade: mild, mod (moderate), sev (severe). Resolved status: ACR was not evident after steroid administration. Etiology: Status of native intestine of the patient; RA+SB, Short bowel syndrome due to resection of small bowel with congenital rotation abnormality; Hir, Hirshpring's disease.

their C-reactive protein (CRP) in peripheral blood increased to >1.0 mg/10^{-1} l, endoscopic examination was performed.

Along with clinical evaluation, pathological examination was performed. Specifically, every day or every other day from postoperative days 7-20, endoscopic examination including biopsy was performed. After a histological diagnosis of ACR, patients received combined immunosuppressant therapy consisting of tacrolimus (baseline, 20 ng/ml) and methylprednisolone (Table 1).

Multivariate morphometric analysis

Images were obtained by microscopy (PROVIS-AX80; Olympus, Tokyo, Japan). Cytoplasm and cell membranes were stained with fluorescent substances, including fluoroisothiocyanate-labeled streptavidin, phycoerythrin-labeled streptavidin (Vector Laboratories, Burlingame, CA, USA) and Alexa 350 (Invitrogen, Carlsberg, CA, USA), which were used for labeling of surface antigens, and fluorescence intensity was quantitatively measured as relative fluorescence units (RFU).

Nuclei were stained with DAPI for cell counting and to distinguish lymphocytes according to their size and circularity. Obtained images were saved as TIF files, and data were analyzed using CELAVIEW software (Olympus), with individual cell signals expressed in terms of RFU, and morphometric data displayed as stained area and circularity. Individual cell data were represented by pixel intensities of the nucleus and cytoplasm. As a morphological control for analysis of iNKT cells, data for $CD3^+$-stained lymphocytes in the allograft were used for validation of the circularity index. Data sets for individual cells on a single slide were represented by two-dimensional scatter plots based on flow cytometry. Plots were further gated according to fluorescence intensity, size and circularity on the scattergram. Circularity was calculated based on Heywood circularity factor using the formula, $P/(4\pi A)^{1/2}$ [18]. Here, the perimeter (P) of individual cells was divided by the circumference of a circle with the same area (A), with the real circle factor being equivalent to 1.0. As the boundary of a binary image is composed of discrete pixels, IMAQ Vision (National Instruments Corporation, Austin, TX, USA) was used to sub-sample the boundary points to approximate a smoother, more accurate perimeter. The closer the shape of the cross section of cells is to a disk, the closer the Heywood circularity factor is to one. Individual data were expressed as means ± SD.

Sampling and storage of biopsy specimens

All specimens were sampled from the mucosa 5-10 cm from the stoma in the course of endoscopic examination. Reviewed biopsy samples are shown in Table 1. All sampled specimens were subjected to immunohistochemistry for CD3, CD4 and CD8. A total of 282 biopsy specimens (28, 32, 24, 16, 8, 14 and 19 samples from injured regions showing endoscopic findings, and the same number of samples from intact mucosa showing no distinct endoscopic findings from eight individual grafts). As normal controls, we utilized five donors (patients' mothers) for histological examination. Twenty cut sections were prepared for H&E staining and immunohistochemistry and were assessed individually. Residual tissues were stored at −80 °C and were subjected to cytokine production assay.

Diagnosis of ACR

We examined the immunohistology of all specimens and investigated the early histological symptoms of ACR for early immunosuppression before the development of crypt apoptosis. Histology of intestinal grafts was assessed according to previously reported criteria [6,7]. To accurately detect apoptotic bodies, TUNEL staining of graft specimens was also performed. Normal allograft status was defined as the absence of crypt apoptosis. We estimated rejection severity as indeterminate, mild, moderate or severe, according to the criteria of the University of Pittsburgh Group.

Routine immunohistochemistry and counting stained cells

The fluorescent staining method for iNKT cells was as reported previously using the CSA system (DAKO, Gostrup, Denmark) [15]. In this study, we used frozen section samples. For primary reagents, we used monoclonal antibody C15 (TCR-Vα24; Immunotech SA, Marseilles, France). To confirm a diagnosis of ACR, antibodies against CD3, CD4 and CD8 were purchased from DAKO, and DAB staining was performed for signal visualization. Negative controls for primary antibodies were IgG1, IG2a and IgG2b (Cat No. X0931, X0943 and X0944; DAKO).

Microdissection

Microdissection-based sampling was performed using frozen specimens with immunostaining. Serial 4-μm sections were cut from embedded tissue. $TCRV\alpha24^+$ cells were separately obtained by manual microdissection using a microdissection system (LM200; Olympus). For routine analysis, genomic DNA was extracted and treated with a REPLI-g Kit (QIAGEN, Hilden, Germany) for amplification of whole genomic DNA. To confirm the dissection of iNKT cells, PCR was performed using the primers for the V24JQ TCR chain according to the method of Oishi *et al.* [19]. PCR amplification was carried out under the following

conditions in a thermal cycler (Perkin-Elmer, Waltham, MA, USA): after denaturation at 95 °C for 2 min, 35 cycles of amplification were performed consisting of denaturation at 94 °C for 40 s, primer annealing at 56 °C for 40 s, and chain elongation at 72 °C for 1 min, followed by a final elongation step at 72 °C for 10 min. Amplicons were electrophoresed on 2.0% agarose gel.

Multiplex-25 bead array assay for ELISA

Graft tissue samples were frozen at −80 °C. Before use, 100 ng of residual tissues were stored in PBS buffer, after which they were added to 1 ml of the appropriate assay diluent provided in the human cytokine multiplex-25 bead array assay kit (Luminex Biosource, Nivelles, Belgium) used for the detection of cytokines [20], specifically IL-4, IL-5, IL-10 and IFN-γ. Antibodies were purchased from Pharmingen (Oxford, UK).

Assay was performed in a 96-well filter plate using all assay components provided in the kit. First, the filter plate was pre-wetted with 200 μl of a working washing solution, and the solution was then aspirated from the wells. Beads (25 μl) were pipetted into each well, and the filter plate wells were washed twice with washing buffer. Incubation buffer (50 μl) and 1:5 diluted fluid intestinal mucosal (30 μg) samples (in 50 μl of buffer as assay diluent) were pipetted into the wells, followed by incubation for 2 h with the beads. Wells were washed, and biotin-conjugated antibody (diluted 1:10) was added for detection. After 1 h, beads were washed again and were incubated for 30 min with streptavidin conjugated to the fluorescent protein R-phycoerythrin (Streptavidin-RPE, diluted 1:10). After washing, beads were analyzed. To validate assay data, whole protein contents were standardized against 200 ng of residual frozen tissue contents after preparation of histologic specimens.

Statistical analysis

All data are expressed as means ± SD. Data analyses were performed by one-way analytic variance (ANOVA) and Spearman's correlation test. All P values were two-sided, and were considered to be statistically significant at <0.05. P values were not adjusted for multiple testing. StatView-J5.0 software (SAS Institute, Cary, NC, USA) was used for all analyses.

Results

Recruitment of TCRVα24-positive invariant T cells to intestinal allograft undergoing ACR

A representative clinical course is shown in Fig. 1a (Patient 2). Histological diagnosis of ACR was made based on the degree of inflammation and the number of apoptotic bodies per ten crypts at 100 postoperative days (Table 1) [6,7]. To identify the phenotypes of inflammatory cells specifically involved in ACR, T/NK-lymphocytic populations in the mucosa of eight allografts were stained using antibodies against CD3, CD4, CD8, CD56 and TCRVα24. Although TCRVα24-positive invariant T cells do not reside in normal human intestine, TCRVα24-positive invariant T cells were observed during ACR and were significantly reduced following high-dose steroid administration (Fig. 1b, Table 1). The specimens studied included

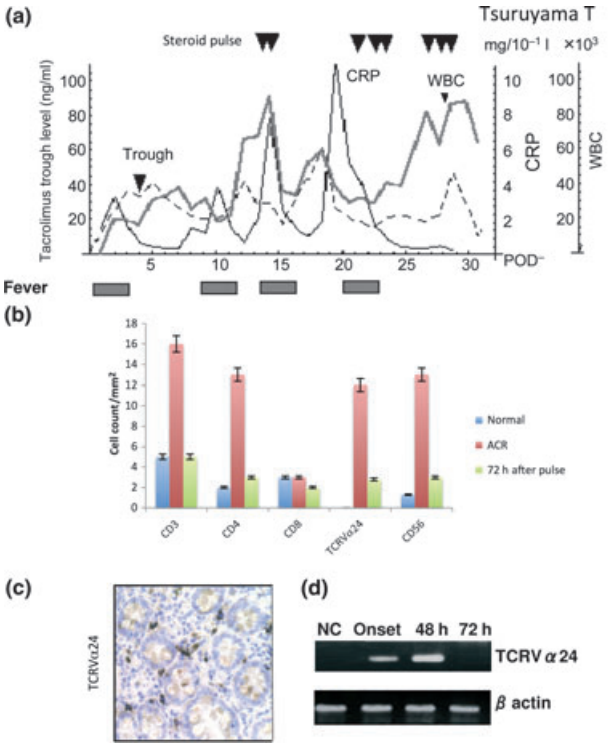

Figure 1 T cells and NK cells in intestinal allografts. (a) Representative clinical course and biopsy data (Patient 2). Trough levels of the immunosuppressive agent tacrolimus are shown. Biopsy was performed eight times during the shown course (Table 1). Solid, dotted, and grey lines indicate C-reactive protein level (mg/10^{-1} l), tacrolimus trough level (ng/ml), and white blood cell (WBC) number (×10^3), respectively. (b) Counts of CD3-, CD4-, CD8-, TCRVα24- and CD56-positive cells per mm^2 in intestinal grafts (mean ± SD, n = 282 from eight grafts). Normal: donor intestine before transplantation. (c) Representative images of combined immunohistochemical staining with anti-TCRVα24 (magnification: left, ×200; center ×600) in intestinal allografts undergoing ACR (Patient 3). Signals were visualized with DAB. (d) RT-PCR assay for detection of recombination of TCRVα24. NC: normal donor intestine; onset: at onset of ACR; 48 h, 72 h: 48 or 72 h after steroid pulse for immunosuppressive therapy. This assay was performed using biopsy specimens obtained from 12 episodes of ACR during examinations performed 72 h after immunosuppression. Three replicates were tested for each biopsy specimen.

five control specimens (from five donor intestines), 16 ACR specimens (from eight engrafted intestines), and 12 specimens obtained 72 h after immunosuppression (from eight engrafted intestines). In addition, PCR analysis for detection of T cell receptor subsets was performed, and recombination of TCRVα24 was confirmed (Fig. 1c). Thus, infiltration of TCRVα24-positive invariant T cells was confirmed to be a feature of ACR in the intestinal allograft.

Quantitative morphometric analysis of iNKT cells

For quantification of histologic observation, we developed morphometric software to count and analyze invariant T cells, which were identified by double staining of TCRVα24-positive invariant T cells with antibodies against TCRVα24 and CD56 (Fig. 2a). Our quantitative morphometric analysis was performed to identify and count double stained cells. First, DAPI-stained nuclei were automatically recognized (Fig. 2b, first image) and counted (Fig. 2b, second image). By detecting the stained area for recognition of cell shape (Fig. 2b, third image), the perimeter of individual cells was measured to estimate circularity (Fig. 2b, fourth image). Two-dimensional scatter plot analysis was performed (Fig. 2c), and gating was performed to exclude nuclei with significantly low- or high-intensity signals, or nuclei with distinct differences from circularity. Cells selected by gating were analyzed, and TCRVα24 signals and CD56 signals of individual cells were further measured. A mean 163 ± 12 nuclei were recognized in each observation of single specimens (a total of 289 specimens from eight intestinal allografts). The results showed that 90% ± 6% (SD) of these invariant cells were positive for CD56 in allografts undergoing ACR (16 episodes of eight allografts). This suggests that most invariant TCRVα24$^+$ cells are iNKT cells.

IL-4 and IL-5 production activity of recruited iNKT cells

Subsequently, quantitative fluorescent morphometric analysis was used to determine which cytokines were produced by iNKT cells in intestinal allografts. The majority of iNKT cells were positive for both IL-4 and IL-5, and the numbers of IL-4$^+$/IL-5$^+$-iNKT cells were significantly lower after steroid administration. In contrast, the number of IFN-γ- or IL-10-producing iNKT cells was very low, and was independent of ACR (16 episodes of 8 allografts, Fig. 3a).

In order to validate the above analysis, multiplex-25 bead array ELISA was retrospectively performed using biopsied samples. For reliable ELISA data, we analyzed samples obtained from grafts during ACR (16 episodes of 8 allografts), in a resolved state at 72 h after immunosuppression (12 episodes in 8 allografts, Table 1), and from normal

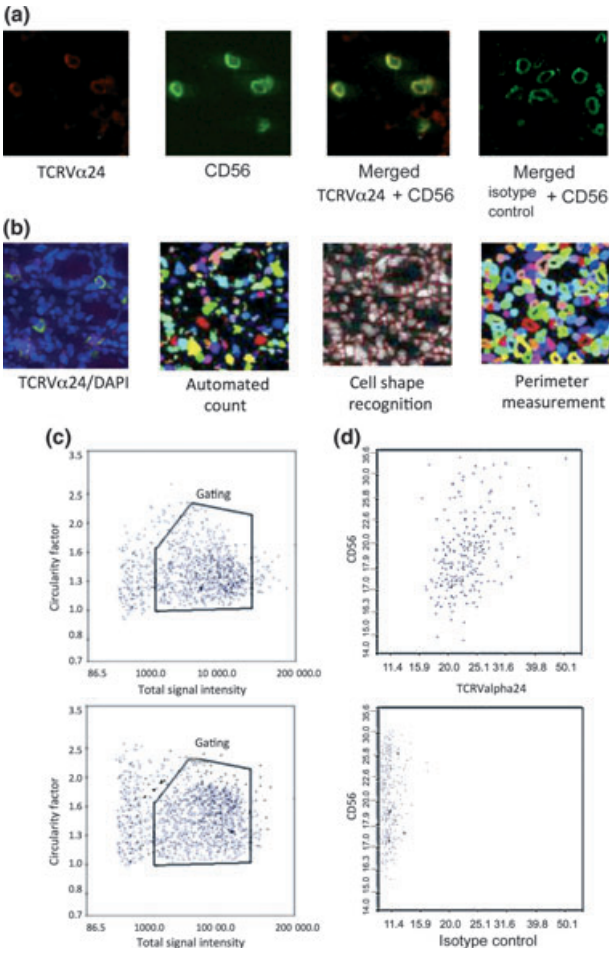

Figure 2 Identification of iNKT cells in intestinal allografts undergoing ACR. (a) Representative serial scheme of automated morphometry of iNKT cells in grafts. Left photo shows anti-TCRVα24 (green with FITC) and anti-CD56 (red with PE) staining. A merged photo of staining with anti-CD56 and an isotype control anti-mouse IgG1 is shown on the right. (b) Process of automated recognition of invariant T cells. Left images show DAPI-staining and TCRVα24-stained cells. Right images show automatically recognized nuclei based on circularity and DAPI signals for a single cell. The perimeter was measured based on the right photo for evaluation of objective circularity. (c) Representative scattergram of gated cells. The vertical axis represents the circularity index, and the horizontal axis represents cell size on the basis of CD56 staining. Circularity index of the CD45R$^+$ lymphoid cells was 1.34 ± 0.12 (SD) (n = 16 episode of ACR shown in Table 1, from the eight allografts) and cells within this range were gated (within boxed area). The cells analyzed in the upper and lower morphometry plots were subjected to TCRVα24 staining and fluorescent staining, respectively (d). (d) Representative scattergram of gated cells (c) doubly stained with FITC-labeled anti-TCRVα24 or isotype control IgG1 and PE-labeled anti-CD56. The vertical axis represents the mean relative fluorescent unit for the FITC-labeled cells, and the horizontal axis represents that of the PE-labeled cells. Data from anti-TCRVα24 and isotype control anti-mouse IgG1 stainings are shown in the upper and lower panels, respectively.

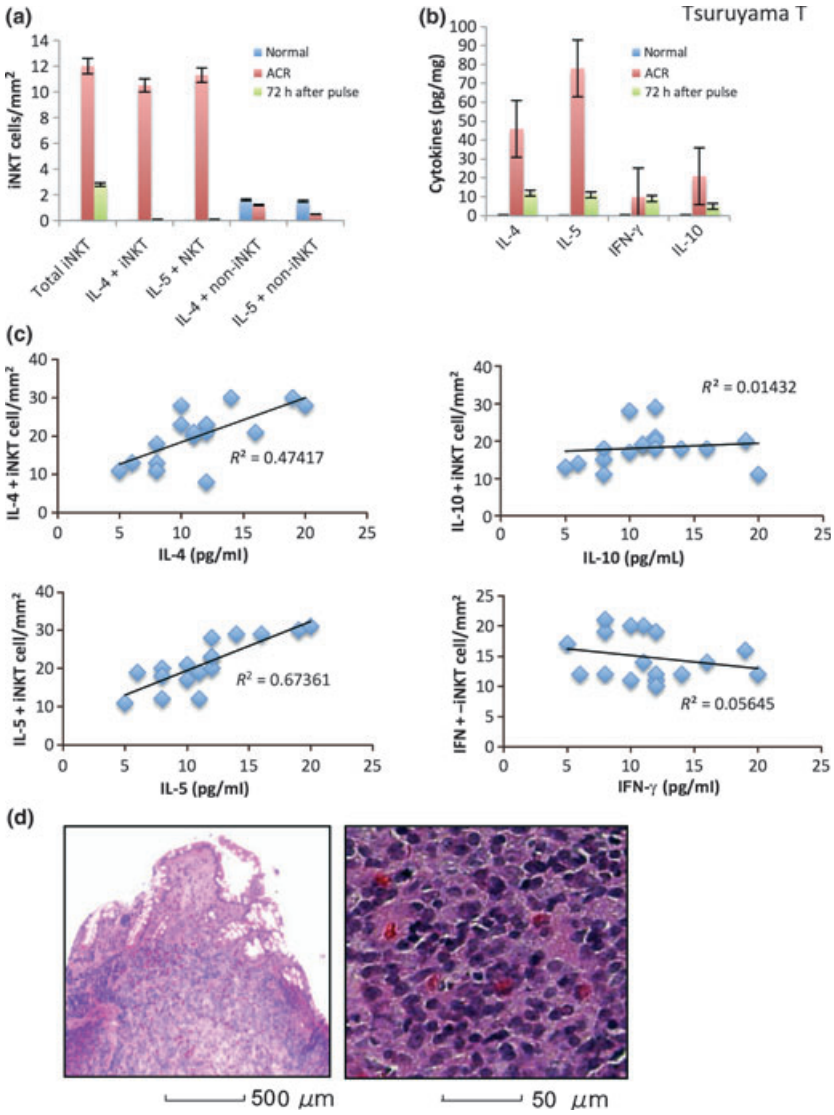

Figure 3 Cytokine production by iNKT cells in grafts. (a) Count of iNKT cells or non-iNKT cells positive for IL-4 and IL-5 in grafts per mm^2. Normal: donor intestine before transplantation [also in (B)]. (b) Total cytokine concentration in sampled tissue. (c) Graphs show plots of amounts of IL-4, IL-5, IFN-γ and IL-10 (pg/mg), counts of IL-4$^+$-, IL-5$^+$-, IFN-γ$^+$- and IL-10$^+$-iNKT cells, and mean counts of IL-4$^+$-, IL-5$^+$-, IFN-γ $^+$- and IL-10$^+$-iNKT cells (per 10 high-power foci). Lines represent linear regression between the amount of cytokine and iNKT cell count. Squares of correlation coefficients in individual analyses are shown next to the lines. (d) H&E staining of grafts with elevated IL-4 and IL-5 levels [magnification: left ×40; right ×400]. Scale bars are shown.

donor intestines before transplantation (n = 6), in which the measured cytokines were above 10 pg/mg. IL-4/IL-5 transiently and significantly increased during ACR; in contrast, neither IFN-γ nor did not IL-10 significantly differ during ACR (16 episodes in 8 allografts, Fig. 3b). Quantitative morphometric analysis was performed using iNKT cells stained with antibodies against IL-4/IL-5 and TCRVα24. The numbers of IL-4$^+$/IL-5$^+$ cells were significantly correlated with total amounts of IL-4/IL-5 in the graft. On the other hand, the numbers of IFN-γ$^+$ iNKT cells and IL-10$^+$ iNKT cells were not significantly correlated with total amounts of IFN-γ or IL-10 in the graft (16 episodes in 8 allografts, Fig. 3c). In parallel with the increases in IL-4 and IL-5, eosinophilic infiltrates were observed at onset of ACR (16 episodes in 8 allografts, Fig. 3d).

Conclusions

We successfully confirmed the presence of iNKT cells in intestinal grafts by multi-color staining. Although immunofluorescent staining identified cytokines and phenotypic surface antigens, overlapping signals on single cells were difficult to distinguish and evaluate without using quantitative morphometry for precise counting of stained cells. This methodology was effective for the quantitative evaluation of the behavior of iNKT cells. By combining the shape based on circularity and the area of DAPI-stained cells, cells could be precisely recognized and distinguished. Using this approach, morphometric analysis was essential for the precise identification of iNKT cells.

In the present study, resident intestinal iNKT cells had the potential to produce IL-4, which antagonizes INF-γ, and contributes to the development of type 2 helper T cells [21]. Higher levels of IL-4 prior to and shortly after transplantation have been reported, and IL-4 may have protective effects on kidney graft survival [22]. Indeed, iNKT cells have been implicated in tolerance in experimental mouse models with induction of chimerism in allogenic cardiac transplant models [14], in acceptance of rat-islet xenografts in mice [23] and in autoimmune diabetes [24]. On the other hand, IFN-γ production remained at low levels relative to normal donor intestine and did not change during the course of ACR development. Although IL-10 production was higher relative to INF-γ production, close correlations were not observed between iNKT cell count and total IL-10 production in the grafts. Among IL-4, IL-10 and IFN-γ, iNKT cells predominantly released IL-4 and may have contributed to suppression of responses by Th1 and cytotoxic T cells. Asaoka *et al.* exhaustively analyzed gene expression profiles in intestinal allografts undergoing ACR. They reported the activation of cytotoxic T lymphocytes (CTLs) in granzyme B/perforin-mediated graft injury. Therefore, release of Th2-related cytokines by iNKT cells may antagonize this activation. In the experimental KO mouse model, the processes involved in tolerance induction are observed in recipient mice with IFN-γ KO iNKT, IL-4 KO iNKT and IL-10 KO iNKT cells [14,25], indicating that tolerance cannot be attributed to a single cytokine, but combined cytokine production may be essential.

Bowel grafts possess their own mucosal immune system, the gut-associated lymphoepithelial tract (GALT), which comprises high endothelial venules (HEV) located in the inter-follicular region (IFR) around the Peyer's patch (PP). GALT immunity is composed of an exquisite balance between activation and suppression through the release of cytokines [26]. At the onset of Crohn's disease, mucosal T cells appear to mount a typical Th1 response that resembles an acute infectious process and is lost with progression to late Crohn's disease. This suggests that mucosal T-cell immunoregulation varies with the course of human inflammatory bowel disease (IBD) [27,28]. Therefore, further assessments are required by monitoring of cytokine production [29–31].

The significance of iNKT cell infiltrates remains unclear. However, it is likely that unknown humoral factors recruit iNKT cells to the graft mucosa in order to suppress allograft rejection. iNKT cells have the ability to release IL-4 and antagonize Th1 and CTL responses [25,31]. However, because the released IL-4 and IL-5 may injure the allograft via eosinophilic enteritis, appropriate immunosuppression is necessary for recovery. We therefore investigated humoral rejection. Humoral and acute vascular rejection (AVR) has been proposed by Ruiz *et al.* [7]. In our cases, distinct AVR was not observed on immunohistochemistry with C4d (data not shown). However, this is an important issue when following the graft, and iNKT cell infiltrates may modulate such ACR via the release of cytokines.

In conclusion, decreases and apoptosis in iNKT cells indicate active rejection. We believe that this study supports clinical intervention in the event of rejection and may lead to better prognosis. A two-dimensional plot is typically used by researchers and provides useful information on the phenotype of stained cells. Our research thus provides an effective technique for pathological diagnosis.

Authorship

TT, SU and HH: designed the research. TT and MM: performed research and study. TT, YF and YY: collected data. TT, HO and SU: analyzed data. TT: wrote the paper.

Funding

This work was supported by a Grant-in-Aid from the Ministry of Education, Culture, Sports, Science and Technology, Japan, Grant No. 12470260. The funder had no role in study design, data collection and analysis, decision to publish or preparation of the manuscript.

References

1. Pirenne J, Hoffman I, Miserez M, *et al.* Selection criteria and outcome of patients referred to intestinal transplantation: an European center experience. *Transplant Proc* 2006; **38**: 1671.
2. Reyes J. Intestinal transplantation for children with short bowel syndrome. *Semin Pediatr Surg* 2001; **10**: 99.
3. Vanderhoof JA. Short bowel syndrome in children and small intestinal transplantation. *Pediatr Clin North Am* 1996; **43**: 533.
4. Avitzur Y, Grant D. Intestine transplantation in children: update 2010. *Pediatr Clin North Am* 2010; **57**: 415. Table of contents.
5. Goulet O, Sauvat F. Short bowel syndrome and intestinal transplantation in children. *Curr Opin Clin Nutr Metab Care* 2006; **9**: 304.
6. Wu T, Abu-Elmagd K, Bond G, Nalesnik MA, Randhawa P, Demetris AJ. A schema for histologic grading of small intestine allograft acute rejection. *Transplantation* 2003; **75**: 1241.
7. Lee RG, Nakamura K, Tsamandas AC, *et al.* Pathology of human intestinal transplantation. *Gastroenterology* 1996; **110**: 1820.

8. Asaoka T, Island ER, Tryphonopoulos P, *et al.* Characteristic immune, apoptosis and inflammatory gene profiles associated with intestinal acute cellular rejection in formalin-fixed paraffin-embedded mucosal biopsies. *Transpl Int* 2011; **24**: 697.
9. Taniguchi M, Harada M, Kojo S, Nakayama T, Wakao H. The regulatory role of Valpha14 NKT cells in innate and acquired immune response. *Annu Rev Immunol* 2003; **21**: 483.
10. Ruiz P, Bagni A, Brown R, *et al.* Histological criteria for the identification of acute cellular rejection in human small bowel allografts: results of the pathology workshop at the VIII International Small Bowel Transplant Symposium. *Transplant Proc* 2004; **36**: 335.
11. Exley M, Porcelli S, Furman M, Garcia J, Balk S. CD161 (NKR-P1A) costimulation of CD1d-dependent activation of human T cells expressing invariant V alpha 24 J alpha Q T cell receptor alpha chains. *J Exp Med* 1998; **188**: 867.
12. Dellabona P, Padovan E, Casorati G, Brockhaus M, Lanzavecchia A. An invariant V alpha 24-J alpha Q/V beta 11 T cell receptor is expressed in all individuals by clonally expanded CD4-8- T cells. *J Exp Med* 1994; **180**: 1171.
13. Spada FM, Koezuka Y, Porcelli SA. CD1d-restricted recognition of synthetic glycolipid antigens by human natural killer T cells. *J Exp Med* 1998; **188**: 1529.
14. Onzuka T, Tomita Y, Shimizu I, *et al.* Role of the cytokine profiles produced by invariant natural killer T cells in the initial phase of cyclophosphamide-induced tolerance. *Transplantation* 2008; **86**: 1301.
15. Tachibana T, Onodera H, Tsuruyama T, *et al.* Increased intratumor Valpha24-positive natural killer T cells: a prognostic factor for primary colorectal carcinomas. *Clin Cancer Res* 2005; **11**: 7322.
16. O'Keeffe J, Doherty DG, Kenna T, *et al.* Diverse populations of T cells with NK cell receptors accumulate in the human intestine in health and in colorectal cancer. *Eur J Immunol* 2004; **34**: 2110.
17. Fujimoto Y, Uemoto S, Inomata Y, *et al.* Small bowel transplantation using grafts from living-related donors. Two case reports.. *Transpl Int* 2000; **13**(Suppl. 1): S179.
18. Friel J, Grande J, Hetzner D. *Practical Guide to Image Analysis*. ASM International: Warrensville Hts., OH, 2000: 157 pp.
19. Oishi Y, Sakamoto A, Kurasawa K, *et al.* CD4-CD8- T cells bearing invariant Valpha24JalphaQ TCR alpha-chain are decreased in patients with atopic diseases. *Clin Exp Immunol* 2000; **119**: 404.
20. Heijmans-Antonissen C, Wesseldijk F, Munnikes RJ, *et al.* Multiplex bead array assay for detection of 25 soluble cytokines in blister fluid of patients with complex regional pain syndrome type 1. *Mediators Inflamm* 2006; **2006**: 28398.
21. Paul WE, Seder RA. Lymphocyte responses and cytokines. *Cell* 1994; **76**: 241.
22. Karczewski J, Karczewski M, Glyda M, Wiktorowicz K. Role of TH1/TH2 cytokines in kidney allograft rejection. *Transplant Proc* 2008; **40**: 3390.
23. Ikehara Y, Yasunami Y, Kodama S, *et al.* CD4(+) Valpha14 natural killer T cells are essential for acceptance of rat islet xenografts in mice. *J Clin Invest* 2000; **105**: 1761.
24. Hong S, Wilson MT, Serizawa I, *et al.* The natural killer T-cell ligand alpha-galactosylceramide prevents autoimmune diabetes in non-obese diabetic mice. *Nat Med* 2001; **7**: 1052.
25. Seino KI, Fukao K, Muramoto K, *et al.* Requirement for natural killer T (NKT) cells in the induction of allograft tolerance. *Proc Natl Acad Sci U S A* 2001; **98**: 2577.
26. Neurath MF, Finotto S, Glimcher LH. The role of Th1/Th2 polarization in mucosal immunity. *Nat Med* 2002; **8**: 567.
27. Kugathasan S, Saubermann LJ, Smith L, *et al.* Mucosal T-cell immunoregulation varies in early and late inflammatory bowel disease. *Gut* 2007; **56**: 1696.
28. Heller F, Fuss IJ, Nieuwenhuis EE, Blumberg RS, Strober W. Oxazolone colitis, a Th2 colitis model resembling ulcerative colitis, is mediated by IL-13-producing NK-T cells. *Immunity* 2002; **17**: 629.
29. Fuss IJ, Heller F, Boirivant M, *et al.* Nonclassical CD1d-restricted NK T cells that produce IL-13 characterize an atypical Th2 response in ulcerative colitis. *J Clin Invest* 2004; **113**: 1490.
30. van Dieren JM, van der Woude CJ, Kuipers EJ, *et al.* Roles of CD1d-restricted NKT cells in the intestine. *Inflamm Bowel Dis* 2007; **13**: 1146.
31. Kim CH, Johnston B, Butcher EC. Trafficking machinery of NKT cells: shared and differential chemokine receptor expression among V alpha 24(+)V beta 11(+) NKT cell subsets with distinct cytokine-producing capacity. *Blood* 2002; **100**: 11.